

## Characteristics of DBD Air Jet under High Temperature and High Pressure for Combustion Assist in an Internal Engine

H. Nishiyama<sup>1</sup>, H. Asano<sup>2</sup>, S. Murakawa<sup>2</sup>, H. Takana<sup>1</sup>, and T. Nakajima<sup>1</sup>

<sup>1</sup>Institute of Fluid Science, Tohoku University, Sendai, 980-8577, Japan, nishiyama@ifs.tohoku.ac.jp

<sup>2</sup>Graduate School Engineering Tohoku University, Sendai, 980-857, Japan, asano@paris.ifs.tohoku.ac.jp

**Abstract:** Experimental analysis of DBD plasma flow was conducted for plasma assisted combustion in an internal engine under high temperature and high pressure. Fundamental characteristics of discharge such as the oxygen radical, ozone productions and energy efficiency for various operating conditions were discussed in detail.

**Keywords:** Plasma, DBD, Air Plasma, Plasma assisted combustion

### 1. Introduction

Recently, plasma has been applied in various fields. Plasma has a multi-functions with high energy density, high controllability by electromagnetic field and chemical high reactivity. In nonequilibrium plasma, active species such as radicals, excited species and charged particles are effectively generated by high energy electron impact reactions. Oxygen radical and ozone in plasma-generated active species have strong oxidation potential and play an important role in combustion enhancement [1]-[8].

However, most of researches on nonequilibrium plasma flow were conducted under atmospheric pressure condition for many applications. Fundamental characteristics of nonequilibrium plasma under high temperature and high pressure condition as in the internal engines have not been clarified in detail.

The purpose of this research is to clarify experimentally the effect of temperature, pressure and applied voltage on radical production in DBD air plasma flow and energy coupling efficiency for plasma assisted combustion in an internal engine.

### 2. Experimental apparatus and measurement

Figure 1 shows the schematic of experimental apparatus. Experimental device consists of power supplies, plasma torch, gas supply section and chamber. Plasma torch has coaxial annulus geometry. Voltage is applied to the inner electrode and the outer electrode is grounded. The dielectric is attached only inner surface of outer electrode. The inner electrode has diameter of 6.0 mm and the inner diameters and thickness of a dielectric are 7.5 mm and 0.8 mm, respectively. Inner electrode distance is 1.55 mm and the distance between a center electrode and a dielectric is 0.75 mm. Electrode material is copper and dielectric material is quartz, respectively.

Air flow rate introduced to DBD torch is set to 6.0 Sl/min by a massflow controller and air is preheated by a heater. The pressure in the chamber is controlled by adjusting inlet and outlet flow rates in the chamber.

In order to clarify the characteristics of DBD air jet

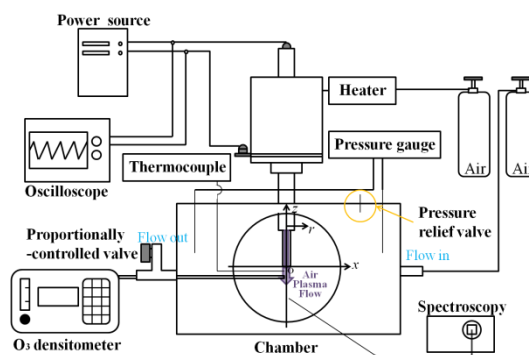


Fig.1 Schematic of experimental apparatus.

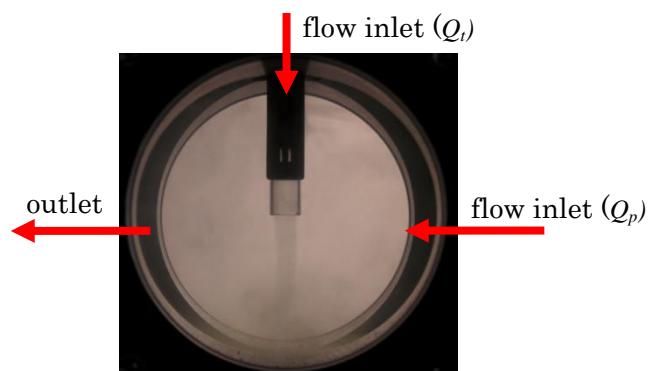


Fig.2 Photograph of flow at  $p = 1.0$  atm,  $Q_i = 6.0$  Sl/min and  $Q_p = 10$  Sl/min.

under high temperature and high pressure, current-voltage characteristics were clarified along with the measurements of gas temperature, spectroscopy, and ozone concentration. Ozone concentration was measured using the ultraviolet absorption-type ozone-concentration meter. Additionally, in order to investigate the influence of the voltage wave forms on radical production, the two kinds of power sources are used. One of the power sources can apply the high voltage sinusoidally at 2.5 kHz. The other one can generate positive high voltage pulse up to 2.0 kHz with the slew rate of 100 V/ns at the duty ratio of 1 %. The maximum applied voltages of sinusoidal

power source and high voltage pulse generator are 20 kV<sub>pp</sub> and 13 kV, respectively.

### 3. Results and discussion

#### 3.1 Visualization of DBD jet

Figure 2 shows the flow pattern of the jet visualized using white smoke without discharge at  $p = 1.0$  atm,  $Q_i = 6.0$  Sl/min and  $Q_p = 10$  Sl/min. In this case, since  $Q_i$  is large enough, the jet is not deflected by the side flow introduced in the chamber for pressure adjustment.

#### 3.2 Discharge characteristics

Figures 3 and 4 show luminescence photograph and discharge waveforms under the same reduced electric field,  $E/N$  at (a)  $p = 1.0$  atm,  $V_{pp} = 10$  kV and (b)  $p = 2.0$  atm,  $V_{pp} = 20$  kV.  $E/N$  can be calculated by the following relation:

$$E/N = \frac{V}{s} \sqrt{\frac{2}{\pi m_e}}$$

where  $V$  is applied voltage;  $s$  is the distance of dielectric and electrode;  $\kappa$  is Boltzmann constant;  $T$  is temperature.  $V_{pp} = 10$  kV and 20 kV are applied sinusoidally at 1.0 atm and 2.0 atm, respectively, so that the same reduced electric field of 272 Td is applied for both cases. Under the same reduced electric field, more discharges occur as found from a current waveform, and luminescence of excitation nitrogen ( $N_2^*$ ) becomes stronger at higher surrounding pressure. This is because higher number density of neutral particles at high pressure produce more number of density of excited species through electron impact excitation.

Figure 5 shows pulsed discharge waveform of voltage at  $p = 1.0$  atm,  $T = 300$  K and  $V = 12$  kV. Positive and negative current flow at rising and falling of the applied voltage, respectively, maximum current of 10 A instantaneously flows at the discharge.

Figure 6 shows the time integrated total input energy and discharge energy per one pulse by pulse generator at applied voltage of 12 kV at 1 atm and 300 K [9]. Total input energy rises up to 5.2 mJ at 2.6  $\mu$ s. Total input power drops to 3 mJ at the fall of applied voltage. On the other hands, the discharge energy increases to 0.58 mJ at  $t = 2.6$   $\mu$ s and to 2.9 mJ at  $t = 7.2$   $\mu$ s. 3 mJ of energy is input to the discharge for 5.0  $\mu$ s. Therefore, the energy coupling efficiency  $\eta$  can be defined as the ratio of total discharge input energy to the maximum total input energy to DBD [10] and the energy coupling efficiency is 56 % in this case.

Figure 7 shows the energy coupling efficiency as a function of  $E/N$  for various operating conditions. There is temperature dependence on energy coupling efficiency strong rather than surrounding pressure. When the temperature is 350 K, the energy coupling efficiency of 50-60 % can be obtained regardless of  $E/N$ . However, in the case of 300 K, the energy coupling efficiency decreases to 30 % with lowering  $E/N$  from 430 Td. For  $E/N$  higher than 430 Td, the energy coupling efficiency of 50-60 % can be obtained.

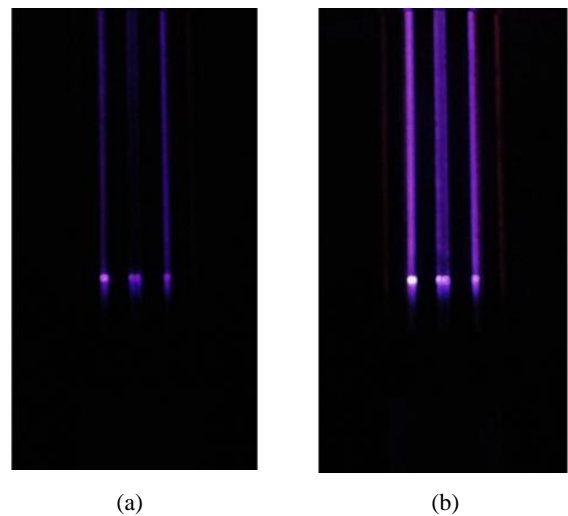


Fig. 3 Discharge luminescence for various pressures at  $E/N = 272$  Td,  $f = 2.5$  kHz. (a)  $p = 1.0$  atm and  $V_{pp} = 10$  kV, (b)  $p = 2.0$  atm and  $V_{pp} = 20$  kV.

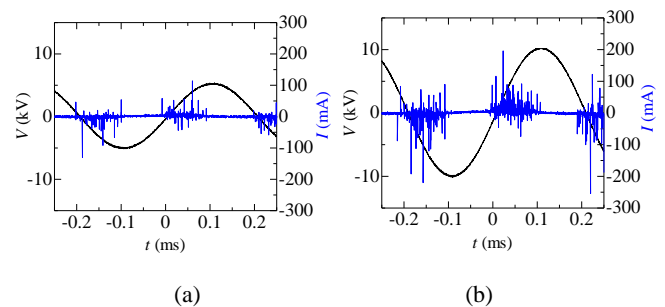


Fig. 4 Discharge waveforms for  $E/N = 272$  Td,  $f = 2.5$  kHz. (a)  $p = 1.0$  atm and  $V_{pp} = 10$  kV, (b)  $p = 2.0$  atm and  $V_{pp} = 20$  kV.

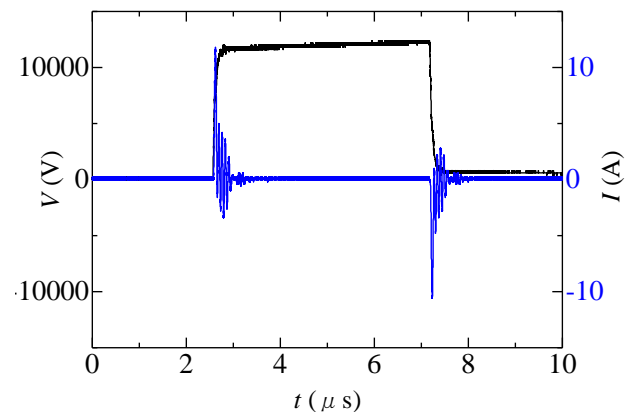


Fig. 5 Discharge waveforms of high voltage pulse at  $p = 1.0$  atm,  $T = 300$  K and  $V = 12$  kV,  $f = 2.0$  kHz.

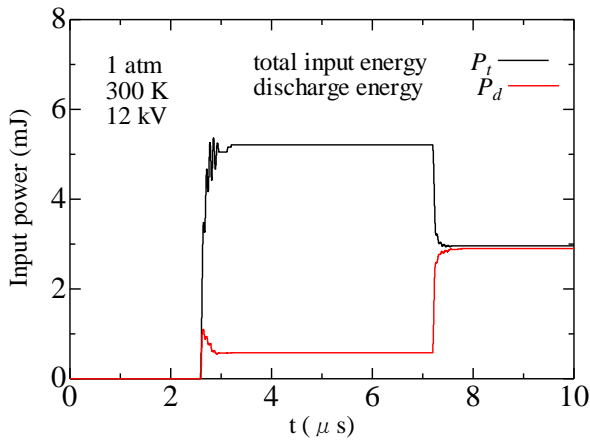


Fig.6 Time integrating of input and discharge energy per one pulse by pulse generator.

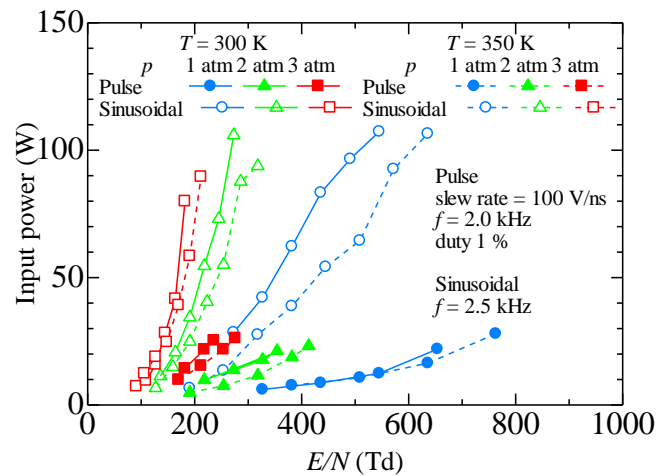


Fig 8 Variation of Input power as a function of  $E/N$ .

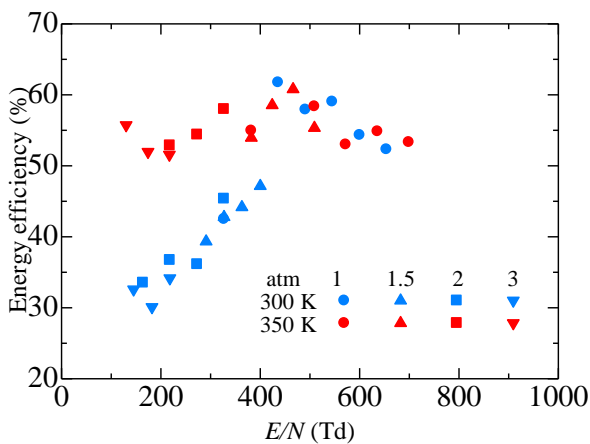


Fig.7 Variation of energy efficiency as a function of  $E/N$ .

Figure 8 shows input power versus  $E/N$  at various pressures and temperatures for sinusoidal or pulsed applied voltage. Input power is smaller for pulsed applied voltage compared with sinusoidal case. Moreover, input power becomes smaller with increase of gas temperature for both power sources

Figure 9 shows the emission intensity of  $N_2^*$  for various  $E/N$  at  $p = 1.0$  atm and  $2.0$  atm,  $T = 300$  K and  $350$  K for sinusoidal or pulsed applied voltage, respectively. The emission intensity of  $N_2^*$  increases exponentially with the increase in reduced electric field, and  $N_2^*$  emission becomes stronger under higher pressure or low temperature due to its higher production rate by electron impact excitation. Compared with the pulsed applied voltage, the  $N_2^*$  emission is intensified for sinusoidal applied voltage.

Figure 10 shows emission intensity of O for various  $E/N$  for sinusoidal or pulse voltage, respectively. The emission of O becomes also high at lower temperature for sinusoidal applied voltage.

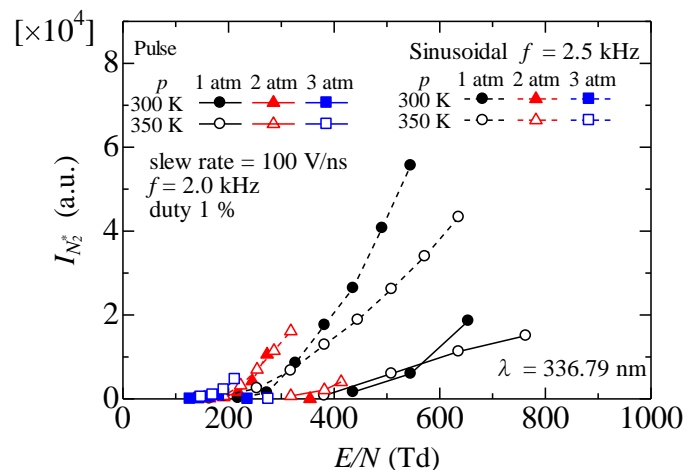


Fig.9 Variation of  $N_2^*$  intensity as a function of  $E/N$ .

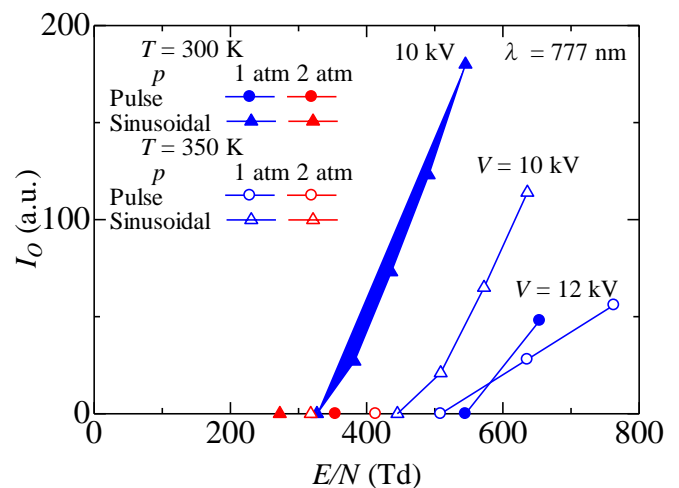


Fig. 10 Variation of O intensity as a function of  $E/N$ .

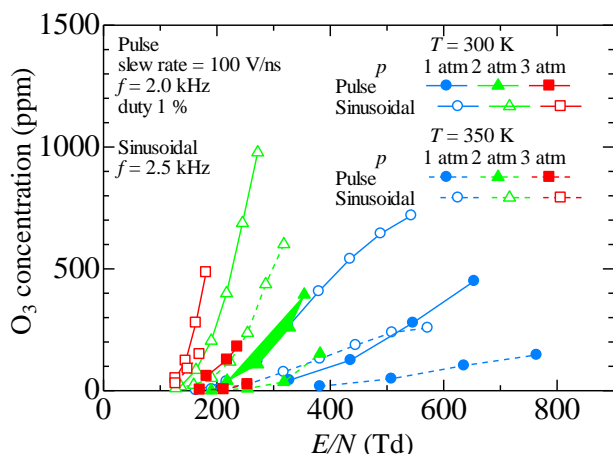


Fig. 11 Variation of ozone concentration as a function of  $E/N$ .

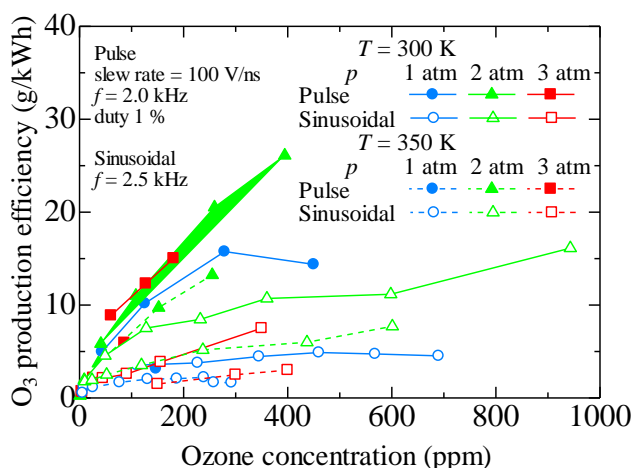


Fig. 12 Variation of ozone production efficiency as a function of ozone concentration.

### 3.3 Ozone production characteristics

Figure 11 shows produced ozone concentration when sinusoidal or pulsed voltage is applied. The dependence of surround pressure and temperature on ozone production for various  $E/N$  is the same for that of  $N_2^*$  and O emission production shown in Fig. 9 and 10. The required  $E/N$  for the ozone production becomes lower with increasing pressure and lowering temperature for both power sources. The maximum of 1000 ppm of ozone is produced at 2 atm, 300 K with sinusoidal applied voltage.

Figure 12 shows ozone production efficiency versus its concentration at various pressures and temperatures for sinusoidal or pulsed applied voltage. Higher ozone generation efficiency can be obtained under high pressure. On the other hand, the efficiency becomes smaller at high temperature. The production efficiency for pulsed applied voltage is higher compared with sinusoidal voltage and it increases with ozone concentration. Although the ozone production efficiency is smaller for sinusoidal applied voltage, the produced ozone concentration is higher than that for pulsed applied voltage.

### 4. Conclusion

To aim at the application of DBD to the plasma assisted combustion in the internal combustion engine, production characteristics of radical and ozone from air are clarified under high pressure and temperature conditions. The results obtained in the present study are summarized follows.

- (1) Energy coupling efficiency has strong temperature dependence rather than surrounding pressure. When temperature is 350 K, the energy coupling efficiency is 50-60 % regardless of  $E/N$ . However, in the case of 300 K, the energy coupling efficiency decreases to 30 % with lowering  $E/N$  from 430 Td.
- (2) Under comparatively high reduced electric field, electronic impact reaction for the formation excited nitrogen and oxygen radical are enhanced under high pressure and low temperature due to higher collision frequency with a neutral particle higher.
- (3) In the case of sinusoidally applied voltage, higher concentration ozone is produced. In the case of pulsed applied voltage, ozone production efficiency is higher.

### Acknowledgements

This study was partly supported by IFS Graduate Student Overseas Presentation Award (2013).

### Reference

- [1] S. M. Starikovskaia, Journal of Physics D, 39 (2006).
- [2] T. Shiraishi, T. Urushihara, M. Gundersen, Journal of Physics D, 42 (2009).
- [3] H. Nishiyama, H. Takana, S. Niikura, H. Shimizu, D. Furukawa, T. Nakajima, K. Katagiri and Y. Nakano, IEEE Transactions on Plasma Science, 4, 36 (2008).
- [4] H. Nishiyama, H. Takana, H. Shimizu, Y. Iwabuchi and Y. Nakano, International Journal of Emerging Multidisciplinary Fluid Sciences, 1, 2 (2009).
- [5] S. Wenting, J. Yiguang, J. Plasma Fusion Res, 89, 4 (2013).
- [6] M. Watanabe, E. Hotta, K. Tanoue, K. Ushimaru, T. Kuboyama, Y. Moriyoshi, J. Plasma Fusion Res, 89, 4 (2013).
- [7] Y. Ikeda, A. Nshiyama, J. Plasma Fusion Res, 89, 4 (2013).
- [8] T. Huiskamp, E.J.M. van Heesch, F.J.C.M. Beckers, W.F.L.M. Hoeben, A.J.M. Pemen, Journal of Physics D, 46, 16 (2013).
- [9] S. Liu and M. Neiger, Journal of Physics D, 36 (2003).
- [10] I. V. Adamovich, M. Nishihara, I. Choi, M. Uddi, and W. R. Lempert, Physics of plasmas. 16, 113505 (2009).